Electronic Supplementary Information

MXene/ZnO flexible freestanding film as dendrite-free support in lithium metal batteries

Yuxi Shen, Ziyan Pu, Yaru Zhang, Yao Chen, Heng Zhang, Nating Wang, Hailong Qiu*, and Yueming Li*

State Key Laboratory of Metastable Materials Science and Technology, College of Materials Science and Engineering, Yanshan University, Qinhuangdao 066004, China E-mail: liyueming@ysu.edu.cn

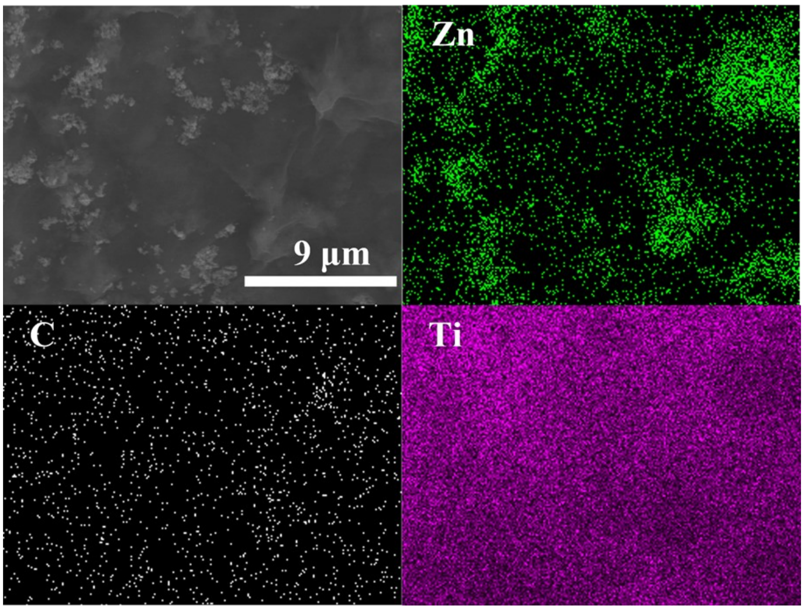

Figure S1 EDS mapping of top surface of MXene/ZnO substrate.

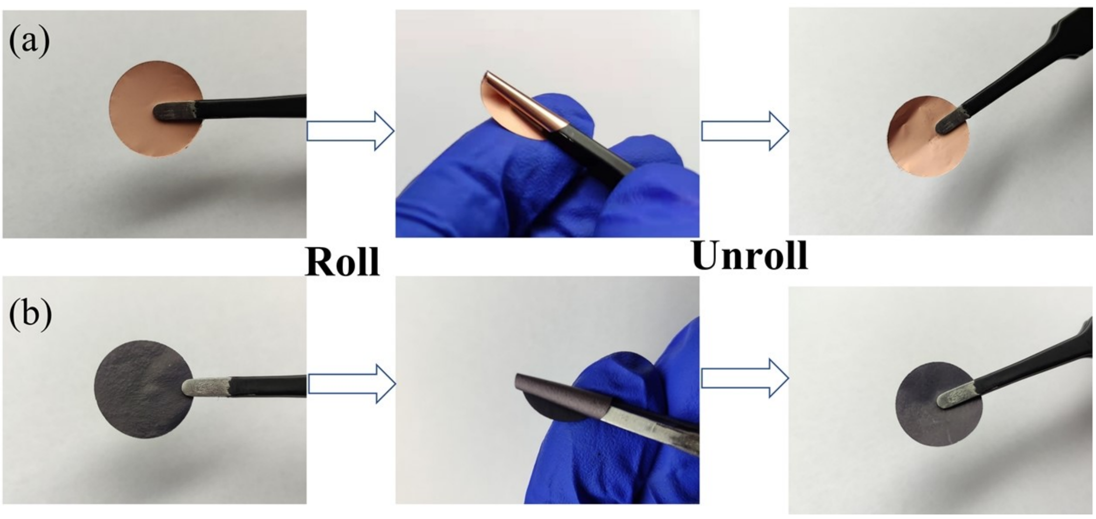

Figure S2 Optical images of roll and unroll of Cu and MXene/ZnO substrates.

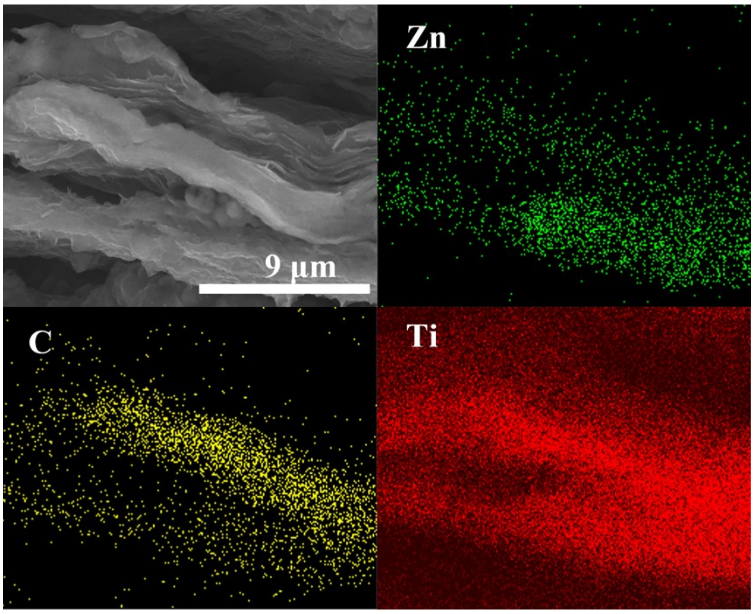

Figure S3 EDS mapping of cross-sectional surface of MXene/ZnO substrate.

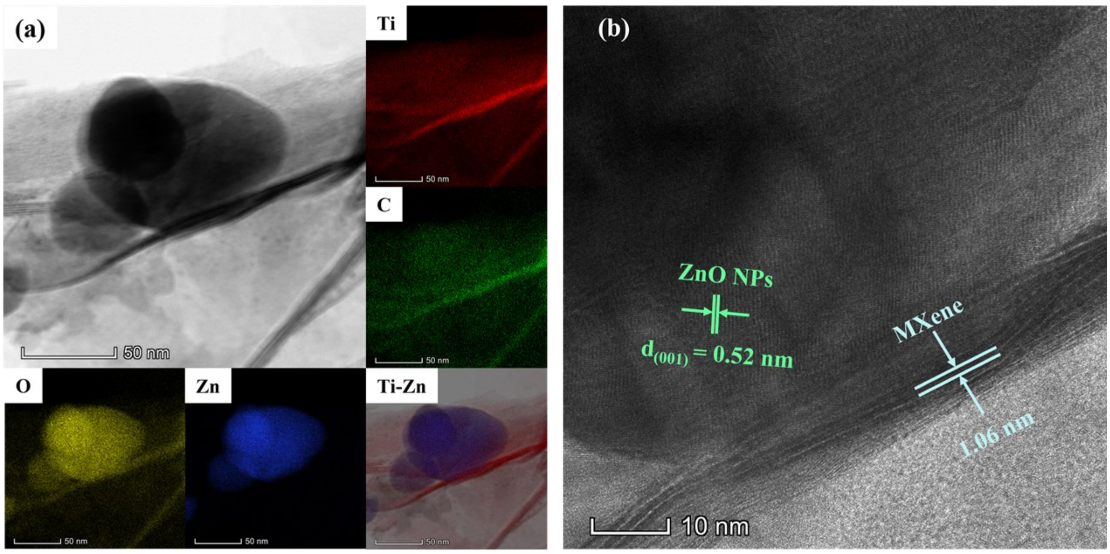

Figure S4 (a) TEM image of MXene/ZnO and corresponding elemental mapping, (b) HRTEM image of MXene/ZnO.

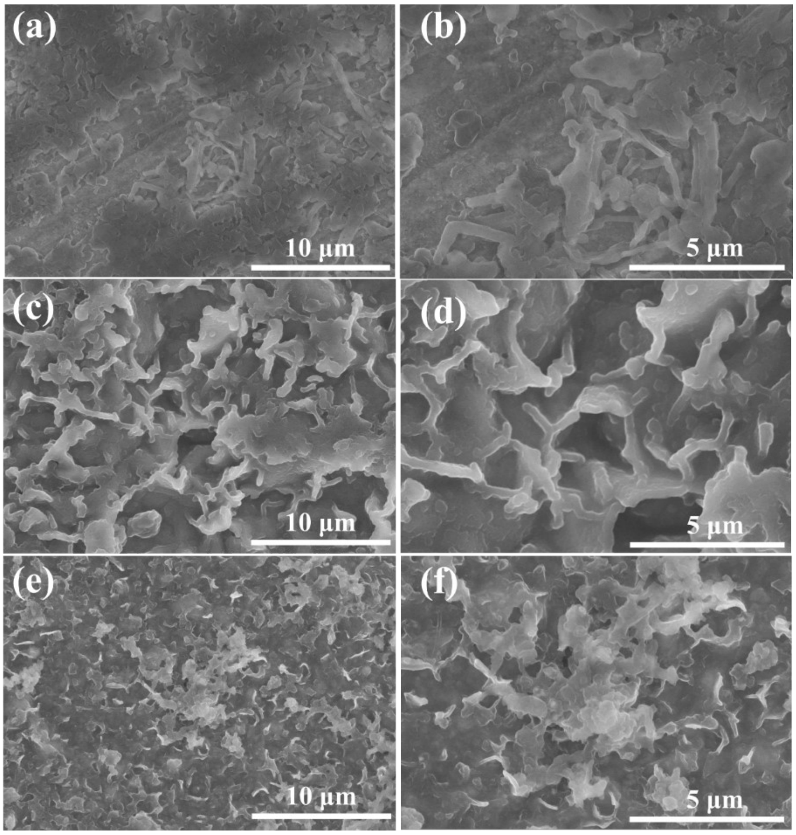

Figure S5 Morphologies of Li plating 0.2 mAh in Cu foil (a-b), MXene substrate (c-d), and MXene/ZnO (e-f).

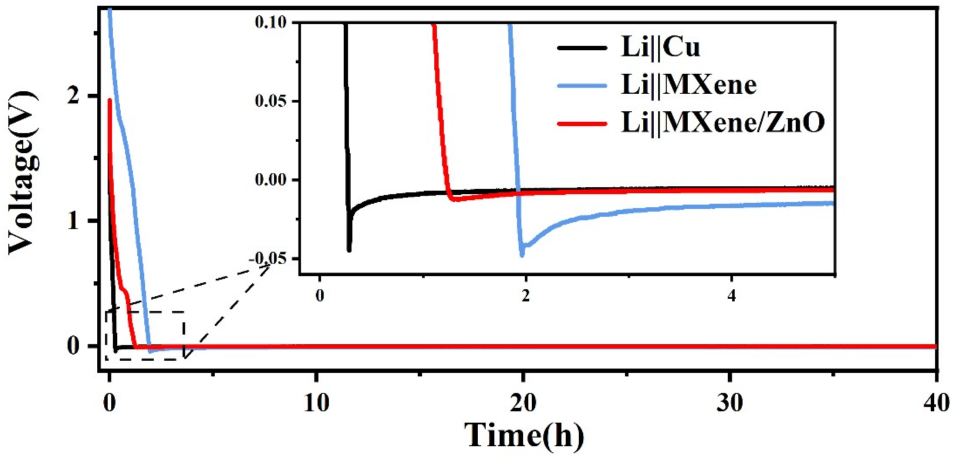

.

Figure S6 Voltage profiles of Li deposition on the Cu, MXene, and MXene/ZnO substrates at the current density of 0.05 mA cm^{-2}.

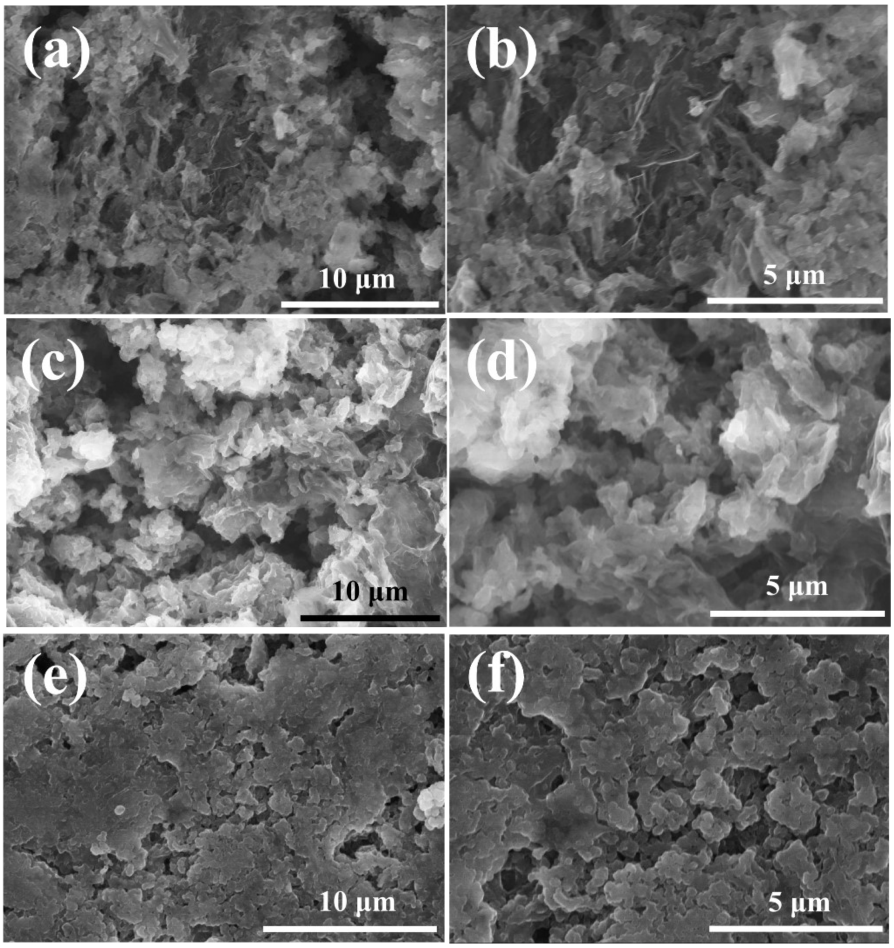

Figure S7 SEM images of Li stripping after 30 cycles (a-b) Cu, (c-d) MXene, and (e-f) MXene/ZnO substrate.

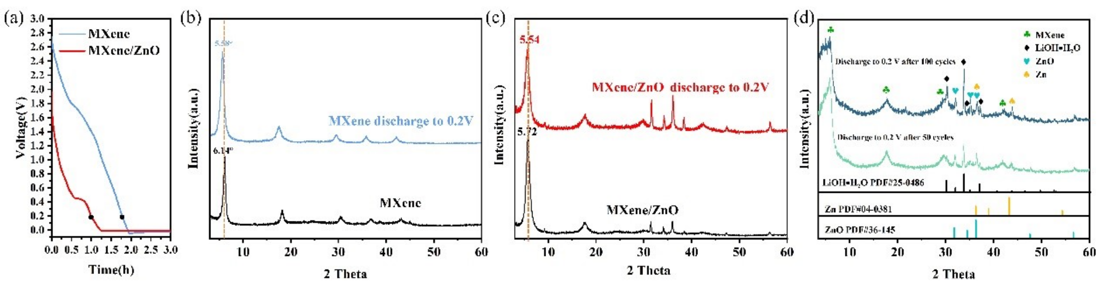

Figure S8 Discharge curves of Li||MXene and Li|| MXene/ZnO cell (a); XRD patterns of MXene (b); and MXene/ZnO (c) substrates when the half-cell was discharged to 0.2 V (vs Li/Li^+). (d) XRD patterns of MXene/ZnO substrates when the half-cell was discharged to 0.2 V (vs Li/Li^+) after 50 and 100 cycles at the current density of 3 mA cm^{-2} and the capacity of 1 mAh cm^{-2}.

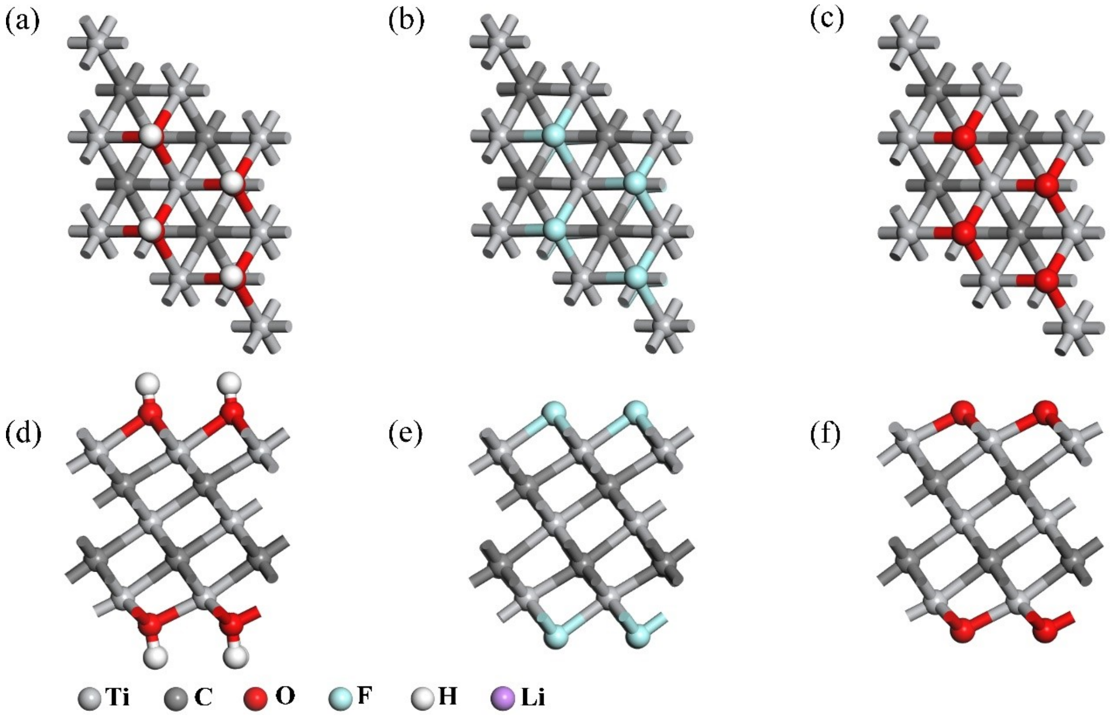

Figure S9 The top and side view of $Ti_3C_2T_x$ with different terminating group.

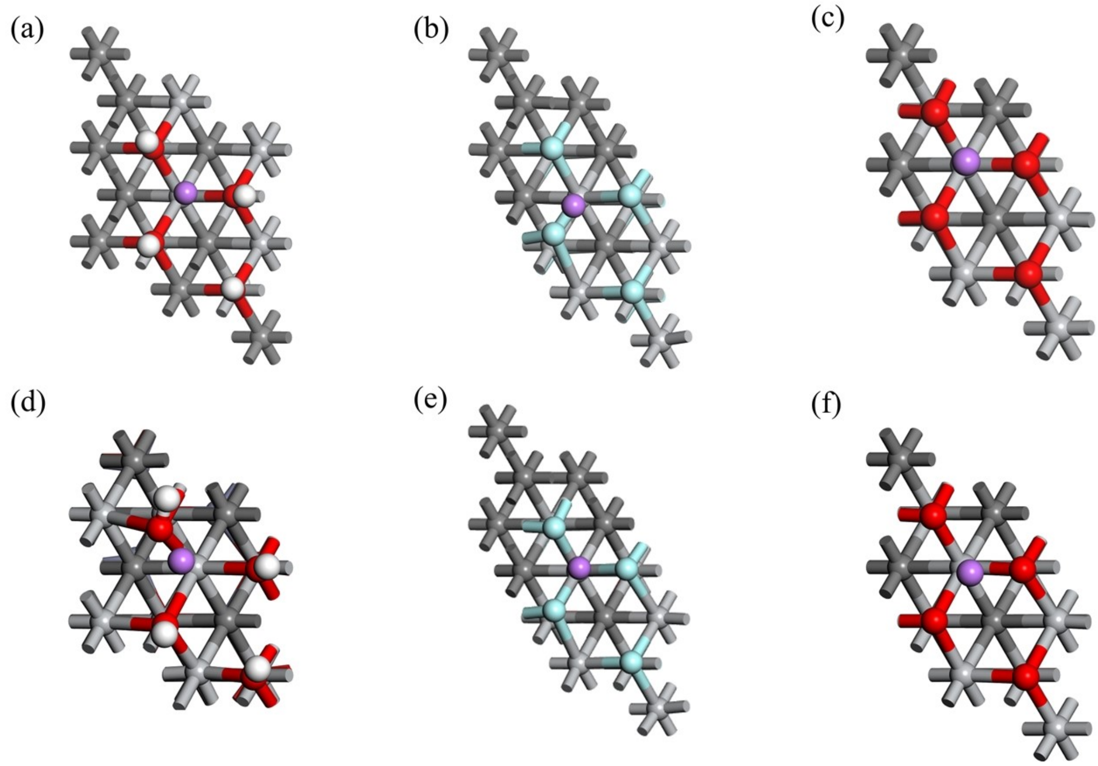

Figure S10 The top view of the optimized site of adsorbed Li on $Ti_3C_2(OH)_2$ (a), $Ti_3C_2F_2$ (b), $Ti_3C_2O_2$ (c), $Ti_3C_2(OH)_2$@ZnO (d), $Ti_3C_2F_2$@ZnO (e), and $Ti_3C_2O_2$@ZnO (f).

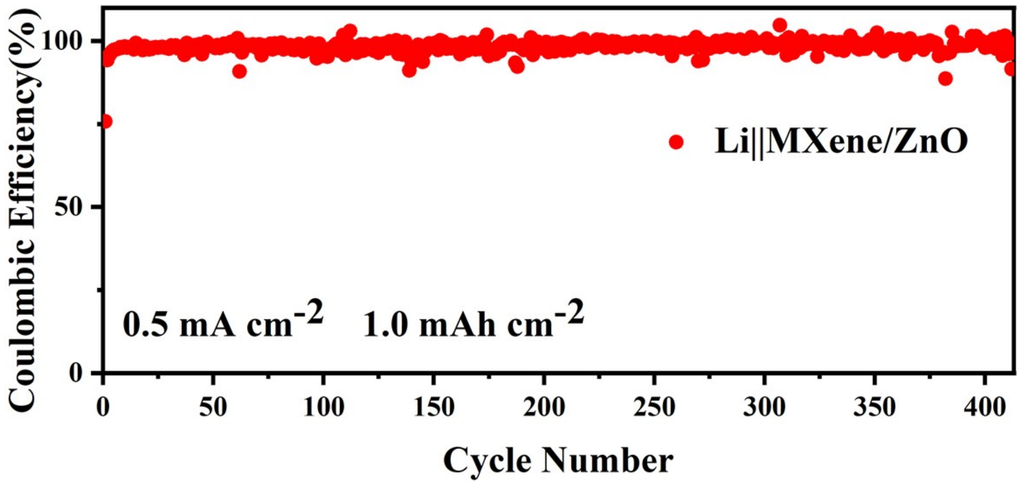

Figure S11 Cycling performance of repeated Li plating/stripping on MXene/ZnO at the current density of 0.5 mA cm^{-2}

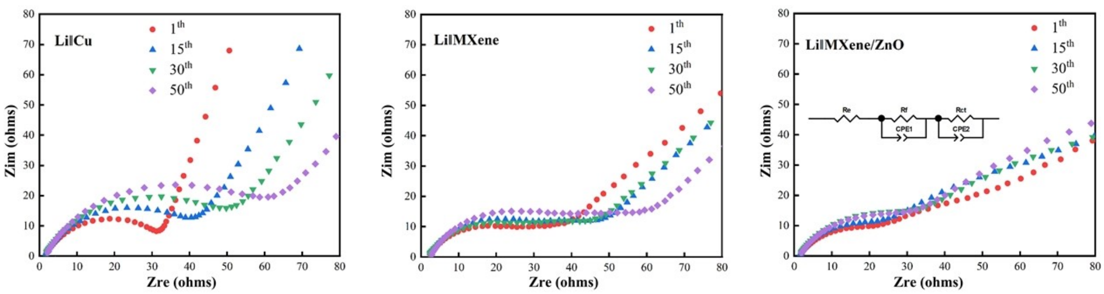

Figure S12 Nyquist plots and equivalent circuit diagram in Li ‖ Cu (a), Li ‖ MXene (b), and Li ‖ MXene/ZnO (c) half-cells at different cycles.

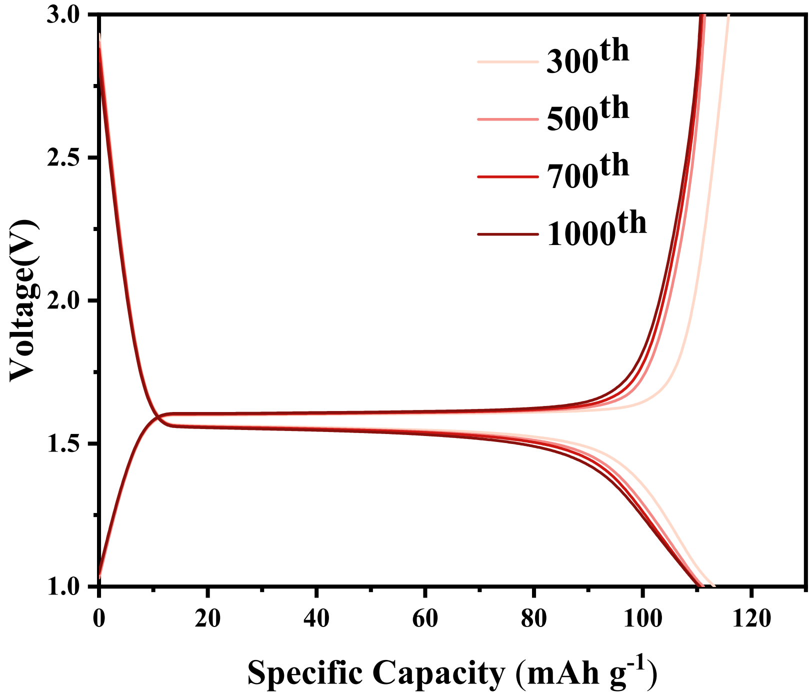

Figure S13 Galvanostatic charge-discharge profiles at 300th,500th,700th and 1000th of LTO || MXene/ZnO@Li full cell.

Table S1 Comparison of the prepared current collector in Li metal half-cell

Materials	Current density & Capacity	Coulombic efficiency	Cycling times	Ref
MXene/ZnO film	0.5mA cm^{-2} 1 mA cm^{-2} 3 mA cm^{-2}	98.3% 97.5% 96.0%	410 330 150	This work
ZnO-CuZn mesh	1 $mAcm^{-2}$, 1 mAh cm^{-2}	97.48%	100	[1]
ZnO in 3D conductive carbon nanofibers	1 $mAcm^{-2}$, 0.5 mAh cm^{-2}	-	200	[2]
ZnO/Carbon nanofibers	1 $mAcm^{-2}$, 1 mAh cm^{-2}	89.8% to 98%	150	[3]
MXene@COFs	1 $mAcm^{-2}$, 2 mAh cm^{-2}	~ 99%	300	[4]
MXene/Graphene farmework	1 $mAcm^{-2}$, 2 mAh cm^{-2}	-	90	[5]
TiO_2 nanoparticles on Ti_3C_2Tx	0.2 $mAcm^{-2}$, 1 mAh cm^{-2}	95.4%	100	[6]
Au@MXene	1 $mAcm^{-2}$, 1 mAh cm^{-2}	99%	200	[7]
Au NPs in rGO	1 $mAcm^{-2}$, 1 mAh cm^{-2}	99.1%	300	[8]
Supersized graphite carbon tubes (S-GCTs)	0.5 $mAcm^{-2}$, 1 mAh cm^{-2}	-	350	[9]
N, O co-doped carbon nanospheres	1 $mAcm^{-2}$, 1 mAh cm^{-2}	97.65 %	275	[10]
Nitrogen-doped hollow porous carbon spheres	1 $mAcm^{-2}$, 1 mAh cm^{-2}	98.5 %	270	[11]
TiN@Cu foam	1 $mAcm^{-2}$, 1 mAh cm^{-2}	~ 98 %	300	[12]
Li_2O on Cu foil	0.25 mA cm^{-2}, 0.25 mAh cm^{-2}	97.8 %	100	[13]
Li_2S@Ni-Nickel foam	1 $mAcm^{-2}$, 1 mAh cm^{-2}	98.1%	100	[14]
Carbon paper/Sn/SnO composite	1 $mAcm^{-2}$, 1 mAh cm^{-2}	98.8 %	300	[15]
3D hierarchical porous Cu@Sn	1 $mAcm^{-2}$, 1 mAh cm^{-2}	98 %	240	[16]
Ultrathin TiO_2 on a Cu current collector	1 $mAcm^{-2}$, 1 mAh cm^{-2}	97.4%	100	[17]
$Cu_{0.7}Zn_{0.3}$/Cu foam	1.5 $mAcm^{-2}$, 1 mAh cm^{-2}	98%	300	[18]
Oxygen vacancy-rich Co_3O_4/nickel foam	1 $mAcm^{-2}$, 1 mAh cm^{-2}	98%	200	[19]
3D porous poly-melamine formaldehyde (PMF)/Li	1 mA cm^{-2}, 1 mAh cm^{-2}	95.8%	300	[20]

Table S2 Comparison of the prepared current collector in lithium metal full cell

Materials	Cathode	Current density	Cycling times	Capacity retention	Ref
MXene/ZnO film	$Li_4Ti_5O_{12}$	5 C	1200	86.7 %	This work
ZnO-CuZn mesh	$LiNi_{1/3}Co_{1/3}Mn_{1/3}O$	1 C	150	94.3 %	[1]
ZnO in 3D conductive carbon nanofibers	$LiFePO_4$	1 C	300	95.7 %	[2]
MXene/Graphene farmework	$Li_4Ti_5O_{12}$	1 C	450	~ 85 %	[5]
Au@MXene	$LiFePO_4$	1 C	200	97.7 %	[7]
TiN@Cu foam	$Li_4Ti_5O_{12}$	2 C	700	93.4 %	[12]
3D porous poly-melamine-formaldehyde (PMF)/Li	$Li_4Ti_5O_{12}$	2 C	1000	~ 92%	[20]
$Ti_3C_2T_x$/g-C_3N_4	$LiFePO_4$	0.5 C	320	85.5 %	[21]
In@$Ti_3C_2T_x$ paper	$LiNi_{0.5}Mn_{1.5}O_4$	200 mA g^{-1}	130	80 %	[22]
Vertically Aligned MXene Nanosheet	$LiFePO_4$	0.5 C	350	85.4 %	[23]

(1 C = 0.175 mAg^{-1} for $Li_4Ti_5O_{12}$, 1 C = 0.17 mAg^{-1} for $LiFePO_4$, 1 C = 0.278 mAg^{-1} for $LiNi_{1/3}Co_{1/3}Mn_{1/3}O$).

References

1. S. Huang, W. Zhang, H. Ming, G. Cao, L. Z. Fan and H. Zhang, *Nano Lett*, 2019, **19**, 1832-1837.
2. Y. Nan, S. Li, Y. Shi, S. Yang and B. Li, *Small*, 2019, **15**, e1903520.
3. Y. Wang, Z. Zhao, W. Zeng, X. Liu, L. Wang, J. Zhu and B. Lu, *J Energy Chem*, 2021, **58**, 292-299.
4. D. Guo, F. Ming, D. B. Shinde, L. Cao, G. Huang, C. Li, Z. Li, Y. Yuan, M. N. Hedhili, H. N. Alshareef and Z. Lai, *Adv Funct Mater*, 2021, **31**, 2101194.
5. H. Shi, C. J. Zhang, P. Lu, Y. Dong, P. Wen and Z. S. Wu, *ACS Nano*, 2019, **13**, 14308-14318.
6. Y. Yan, C. Shu, R. Zheng, M. Li, Z. Ran, M. He, L. Ren, D. Du and Y. Zeng, *J Energy Chem*, 2022, **65**, 654-665.
7. Y. Qian, C. Wei, Y. Tian, B. Xi, S. Xiong, J. Feng and Y. Qian, *Chem Eng J*, 2021, **421**, 129685.
8. W. Y. Diao, D. Xie, Y. F. Li, R. Jiang, F. Y. Tao, H. Z. Sun, X. L. Wu, X. Y. Zhang and J. P. Zhang, *Chem-Eur J*, 2021, **27**, 8168-8177.
9. W. Chen, Y. Hong, Z. Zhao, Y. Zhang, L. Pan, J. Wan, M. Nazir, J. Wang and H. He, *J Mater Chem A*, 2021, **9**, 16936-16942.
10. C. Gao, J. Li, K. Sun, H. Li, B. Hong, M. Bai, K. Zhang, Z. Zhang and Y. Lai, *Chem Eng J*, 2021, **412**, 128721.
11. W. Ye, F. Pei, X. Lan, Y. Cheng, X. Fang, Q. Zhang, N. Zheng, D. L. Peng and M. S. Wang, *Adv Energy Mater*, 2020, **10**, 1902956.

12. Y. Wang, W. Zhang, Y. Qi, S. Wang, P. Liu, X. Wei, Y. Yu, W. Sun, X.-Z. Zhao and Y. Liu, *J Alloy Compd*, 2021, **874**, 159916.
13. Z. Gong, C. Lian, P. Wang, K. Huang, K. Zhu, K. Ye, J. Yan, G. Wang and D. Cao, *Energ Environ Mater*, 2021, DOI: 10.1002/eem2.12243.
14. J. Zhang, Y. Zhou, F. Tu, Y. Ma, H. Zhang, D. Song, X. Shi and L. Zhang, *Chem Eng J*, 2022, **428**, 132510.
15. L. Tan, S. Feng, X. Li, Z. Wang, W. Peng, T. Liu, G. Yan, L. Li, F. Wu and J. Wang, *Chem Eng J*, 2020, **394**, 124848.
16. Z. Luo, C. Liu, Y. Tian, Y. Zhang, Y. Jiang, J. Hu, H. Hou, G. Zou and X. Ji, *Energy Storage Mater*, 2020, **27**, 124-132.
17. L. Tan, X. Li, T. Liu and X. Li, *J Power Sources*, 2020, **463**, 228157.
18. Y. Cheng, X. Ke, Y. Chen, X. Huang, Z. Shi and Z. Guo, *Nano Energy*, 2019, **63**, 103854.
19. Z. Wang, H. Shi, S. Yang, Z. Cai, H. Lu, L. Jia, M. Hu, H. He and K. Zhou, *J Alloy Compd*, 2021, **888**, 161553.
20. L. Fan, H. L. Zhuang, W. Zhang, Y. Fu, Z. Liao and Y. Lu, *Adv Energy Mater*, 2018, **8**, 1703360.
21. F. Zhao, P. Zhai, Y. Wei, Z. Yang, Q. Chen, J. Zuo, X. Gu and Y. Gong, *Adv Sci* 2022, **9**, e2103930.
22. Y. Qian, Y. An, Y. Zhang, C. Wei, B. Xi, S. Xiong and J. Feng, *J Power Sources*, 2022, **520**, 230901
23. Q. Chen, Y. Wei, X. Zhang, Z. Yang, F. Wang, W. Liu, J. Zuo, X. Gu, Y. Yao, X. Wang, F. Zhao, S. Yang and Y. Gong, *Adv Energy Mater*, 2022, **12**, 2200072